

# Design and status of the Mu2e crystal calorimeter

N. Atanov<sup>a</sup>, V. Baranov<sup>a</sup>, C. Bloise<sup>b</sup>, J. Budagov<sup>a</sup>, F. Cervelli<sup>c</sup>, S. Ceravolo<sup>b</sup>, F. Colao<sup>b</sup>, M. Cordelli<sup>b</sup>, G. Corradi<sup>b</sup>, Yu.I. Davydov<sup>a</sup>, S. Di Falco<sup>c</sup>, E. Diociaiuti<sup>b,d</sup>, S. Donati<sup>c,e</sup>, R. Donghia<sup>b,f,\*</sup>, B. Echenard<sup>g</sup>, C. Ferrari<sup>c</sup>, S. Giovannella<sup>b</sup>, V. Glagolev<sup>a</sup>, F. Grancagnolo<sup>h</sup>, D. Hampai<sup>b</sup>, F. Happacher<sup>b</sup>, D. Hitlin<sup>g</sup>, M. Martini<sup>b,i</sup>, S. Miscetti<sup>b</sup>, T. Miyashita<sup>g</sup>, L. Morescalchi<sup>c</sup>, P. Murat<sup>j</sup>, D. Pasciuto<sup>b,i</sup>, E. Pedreschi<sup>c</sup>, G. Pezzullo<sup>k</sup>, F. Porter<sup>g</sup>, F. Raffaelli<sup>c</sup>, A. Saputi<sup>b</sup>, I. Sarra<sup>b,i</sup>, F. Spinella<sup>c</sup>, G. Tassielli<sup>h</sup>, V. Tereshchenko<sup>a</sup>, Z. Usubov<sup>a</sup>, I.I. Vasilyev<sup>a</sup>, A. Zanetti<sup>b</sup>, R.Y. Zhu<sup>g</sup>

<sup>a</sup>Joint Institute for Nuclear Research, Dubna, Russia

<sup>b</sup>Laboratori Nazionali di Frascati dell'INFN, Frascati, Italy

<sup>c</sup>INFN Sezione di Pisa, Italy

<sup>d</sup>Dipartimento di Fisica, Università Tor Vergata, Rome, Italy

<sup>e</sup>Dipartimento di Fisica, Università di Pisa, Italy

<sup>f</sup>Dipartimento di Fisica, Università Roma Tre, Rome, Italy

<sup>g</sup>California Institute of Technology, Pasadena, United States

<sup>h</sup>INFN Sezione di Lecce, Italy

<sup>i</sup>Università Guglielmo Marconi, Rome, Italy

<sup>j</sup>Fermi National Laboratory, Batavia, Illinois, USA

<sup>k</sup>Yale university, New Haven, USA

<sup>l</sup>INFN Sezione di Trieste, Italy

---

## Abstract

The Mu2e experiment at Fermilab searches for the coherent neutrino-less muon to electron conversion in the Coulomb field of an aluminium nucleus. This charged-lepton flavour violating process is characterised by a distinctive signature of a mono-energetic electron ( $\sim 105$  MeV/c) and its observation will be a clear signature of new physics beyond the Standard Model. The Mu2e goal is to improve by four orders of magnitude the search sensitivity with respect to the previous experiments. The Mu2e detector is composed of a tracker, an electromagnetic calorimeter and an external veto for cosmic rays. The calorimeter plays an important role in providing excellent particle identification capabilities, a fast online trigger filter while aiding the track reconstruction capabilities. It consists of 1348 pure CsI crystals divided in two annular disks, each one readout by two large area Silicon Photomultipliers. A large scale prototype has been tested with an electron beam, demonstrating to largely satisfy the Mu2e requirements. At the moment of writing, the crystals and SiPMs production phase is halfway through the completion. An overview of the characterisation tests is reported, together with a description of the final mechanical and electrical design.

**Keywords:** Mu2e, Calorimetry, Pure CsI crystals, SiPMs

**PACS:** 29.40.Mc, 29.40.Vj

---

## 1. Introduction

The Mu2e experiment, aiming to search for the  $\mu$ -e conversion process [1][2], consists of a straw tube tracker and a crystal calorimeter embedded inside the evacuated region of a superconducting solenoid providing a 1 T axial magnetic field in their location. The external region of the solenoid is surrounded by a cosmic ray veto detector. The calorimeter [3] helps the tracker in the identification of  $\sim 105$  MeV/c conversion electrons (CEs), building an efficient trigger, providing particle identification and improving the track reconstruction capabilities. According to Monte Carlo simulation, the calorimeter performance requirements on CEs are as follows: an energy resolution better than 10%; a time resolution below 0.5 ns and a spatial resolution better than 1 cm. The calorimeter design consists of two

disks of 674 un-doped CsI crystals of  $34 \times 34 \times 200$  mm<sup>2</sup> dimension, each readout by two custom large area UV-extended Silicon Photomultipliers (Mu2e SiPMs). Each Mu2e SiPM is an array consisting of two series of 3 monolithic  $6 \times 6$  mm<sup>2</sup> cells connected in parallel [4]. The Front End amplification and HV regulator boards are connected to the SiPM pins while the digitization of the signals is carried out by custom boards located in nearby crates. A radioactive source and a laser system allow setting the energy scale and monitor the fast changes of response and resolution. A long R&D phase [5][6] demonstrated this design option largely satisfies the Mu2e calorimeter requirements. Updated results of a large area calorimeter prototype test beam are reported in the following sections.

## 2. Prototype performance

A Module-0 calorimeter prototype (Fig. 1) has been built to resemble as much as possible the final disk mechanical design.

---

\*Corresponding author

Email address: raffaella.donghia@lnf.infn.it ()

31 Its construction was used to validate the assembly procedure  
 32 and evaluate the detector performance with an electron beam in  
 33 the energy range of 60-120 MeV at the Beam Test Facility [7]  
 34 of the INFN Laboratory in Frascati. The prototype is composed  
 35 by 51 crystals and 102 Mu2e SiPMs produced and qualified  
 36 during the pre-production phase [8][9].



Figure 1: Pictures of Module-0 front view during assembly : mechanical structure (top left), crystals assembly (bottom left) and final version (right).

37 Similarly to the calorimeter disk, Module-0 is a structure of  
 38 staggered crystals with a size large enough to contain most of  
 39 the electromagnetic shower for 105 MeV electrons. Energy and  
 40 time measurements were obtained using the beam impinging on  
 41 the calorimeter surface both at 0 and at 50 degrees, which is  
 42 the expected CEs incidence angle. Data acquisition lasted one  
 43 week in May 2017, by triggering both on beam and cosmic rays  
 44 (CRs) data and acquiring at 1 GHz sampling rate.

## 45 2.1. Energy resolution

46 After selecting single-particle events, digitized waveforms  
 47 are integrated in a 200 ns wide time window around the maximum  
 48 amplitude, in order to evaluate the collected charge. To  
 49 equalize the response of each channel, the charge deposition  
 50 from CRs minimum ionizing particles is determined and then  
 51 compared with the Monte Carlo (MC) expected energy deposition.  
 52 The calibration statistical uncertainty for each channel is  
 53 of around 0.5%. After equalization, the energy scale is set by  
 54 comparing the reconstructed charge in the whole detector ( $Q_{rec}$ )  
 55 with the total energy deposited by a 100 MeV electron, as evaluated  
 56 by a Geant-4 based Monte Carlo simulation (MC). A good  
 57 linearity in response is observed with an energy scale factor  
 58  $E_{sc} = (12.07 \pm 0.11)$  pC/MeV. Such calibration is then applied  
 59 to all signals to obtain the reconstructed energy,  $E = Q_{rec}/E_{sc}$ .

A log-normal fit is applied to each reconstructed energy distribution and the resolution ( $\sigma_E/E$ ) is evaluated as the ratio between the sigma and the peak. An energy resolution of  $\sim 5.3\%$  (7.4%) is obtained at 100 MeV beam energy for 0 (50) degrees impinging angle. The energy resolution for all the test configurations is reported in Figure 2, together with MC simulation results. A very good agreement is shown. The dependence of the energy resolution as a function of the deposited energy  $E_{dep}$

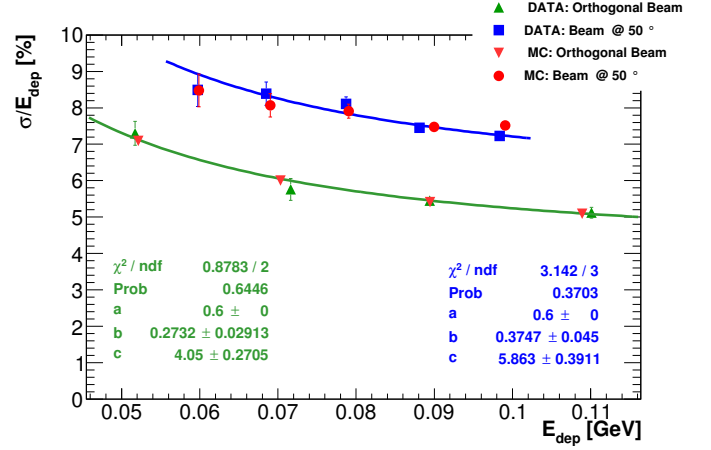


Figure 2: Energy resolution as a function of the deposited energy in Module-0. Green (blue) points are the results for the beam impinging at 0 (50) degrees. Red points are the results from MC simulation.

for single particle events has been parametrized by the function:

$$\frac{\sigma_E}{E_{dep}} = \frac{a}{\sqrt{E_{dep}[\text{GeV}]}} \oplus \frac{b}{E[\text{GeV}]} \oplus c, \quad (1)$$

where  $a$  represents the stochastic term,  $b$  the noise term and  $c$  the constant term. The fit resulted to be rather insensitive to the stochastic term, so that it has been fixed to 0.6%, corresponding to the measured light yield value of 30 pe/MeV [9]. The resolution deterioration at the CE average incidence angle of 50° is dominated by the increase of the leakage contribution from the Module-0 front face.

## 67 2.2. Timing Resolution

68 The signal time is determined by fitting the waveform leading edge with an asymmetric log-normal function and applying the constant fraction (CF) method. The fit range and CF have been varied to optimize the timing resolution. The optimized CF value found is at 5% of the amplitude peak.

The time resolution for a single sensor is evaluated as  $\sigma(\Delta T)/\sqrt{2}$ , where  $\sigma$  is extracted by applying a Gaussian fit on the time difference ( $\Delta T$ ) between the two readout SiPMs of the same crystal. A single sensor resolution of  $\sim 130$  ps is obtained for 100 MeV electron beam at 0 degree. Since the sampling frequency of the Mu2e digitizer boards is of 200 Msps, the waveforms were offline re-sampled in 5 ns bins. Figure 3 shows the time resolution as a function of the highest crystal energy deposit at different beam energies, for both 1 Gsps and 200 Msps sampling rates. A time resolution deterioration smaller than 30% is obtained, which is negligible with respect to the Mu2e calorimeter requirements.

## 3. Production phase

On March 2018, we started receiving the final CsI crystals from the companies SICCAS and Saint Gobain (SG), in batches of 60 samples per month. Mechanical problems on SG crystals

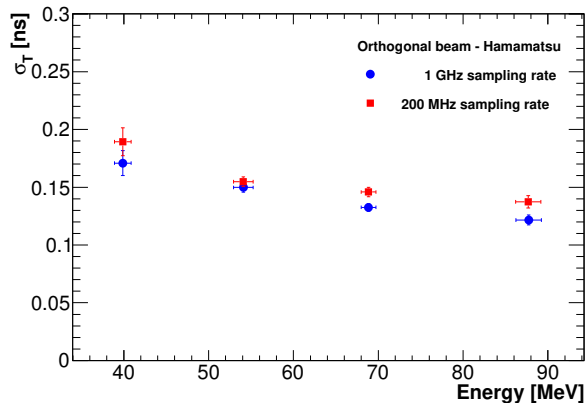


Figure 3: Time resolution as a function of the deposited energy in the highest energetic crystal, considering both the 1 GHz (blue points) and 200 MHz (red square) sampling rates.

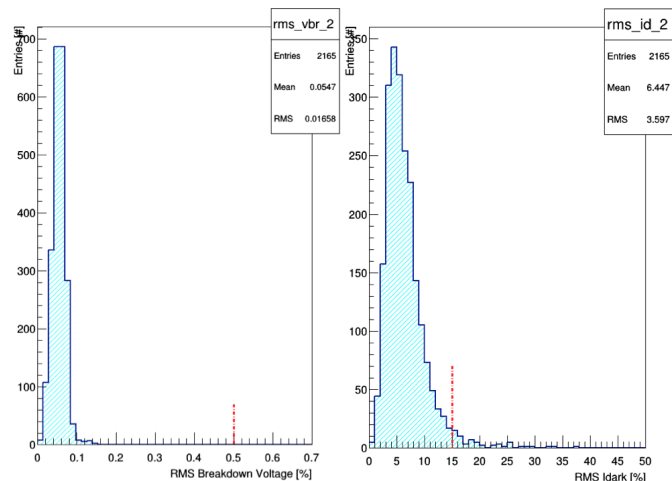


Figure 5: RMS distributions of the  $V_{br}$  and  $I_d$  measurements over the six cells of the Mu2e-SiPMs arrays.

89 delayed their production. At the moment of writing, 900 crystals  
 90 have been already tested in dedicated automatised custom<sup>116</sup>  
 91 stations. The mechanical properties (lengths, perpendicularity<sup>117</sup>  
 92 and parallelism between faces) are evaluated using a CMM ma-<sup>118</sup>  
 93 chine. Crystals outside the dimensional specification with a tol-<sup>119</sup>  
 94 erance of 0.1 mm are rejected. The other stations are used to<sup>120</sup>  
 95 measure the crystal optical properties, after wrapping each of<sup>121</sup>  
 96 them with 150  $\mu\text{m}$  Tyvek foil. A PMT readout is used. The<sup>122</sup>  
 97 crystals are exposed to a  $^{22}\text{Na}$  source, which emits 511 keV<sup>123</sup>  
 98 photons, and the Light Yield (LY), the Longitudinal Response<sup>124</sup>  
 99 Uniformity (LRU) and the resolution are measured. Figure 4<sup>125</sup>  
 100 shows the results on LY (left) and LRU (right) measurements.<sup>126</sup>  
 101 Less than 1% of the production has been rejected due to optical  
 properties.

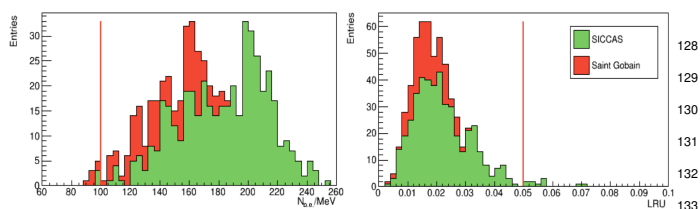


Figure 4: LY and LRU of about half of the crystal production.

102 In the same period, 2700 out of the 4000 Mu2e-SiPM from  
 103 Hamamatsu have been characterised. For each Mu2e SiPM, the  
 104 breakdown voltage,  $V_{br}$ , the dark current,  $I_d$ , and the  $gain \times PDE$   
 105 are measured for all the six  $6 \times 6 \text{ mm}^2$  cells inside the sensor  
 106 array. The spread of these measurements over the six cells  
 107 is also measured and 2% of the SiPMs have been rejected due to  
 108 a large RMS on the dark current ( $> 5\%$ ). The test is performed  
 109 at three different temperatures:  $0^\circ\text{C}$ ,  $10^\circ\text{C}$  and  $20^\circ\text{C}$ . Figure 5  
 110 shows the RMS spread value of the  $V_{br}$  and  $I_d$  measurements at  
 111  $20^\circ\text{C}$ , on left and right plot respectively.

112 The procurement proceeded with monthly batches of 280,<sup>134</sup>  
 113 SiPMs each. Out of each batch, we randomly select 15 units<sup>135</sup>  
 114 to test their Mean Time to Failure (MTTF). The Mu2e require-<sup>136</sup>

ment is a MTTF of at least 1 million hours when operating at  
 $0^\circ\text{C}$ . To accelerate the measurement, the sensors are tested for  
 18 days with a burn-in at  $65^\circ\text{C}$ . No damage has been observed  
 so far, so that the Mu2e SiPMs experimentally demonstrate an  
 MTTF larger than 10 million hours. For each batch, additional  
 5 pieces are randomly chosen to carry out the neutron radiation  
 hardness test. These sensors are exposed to a total fluence of  
 $1.2 \times 10^{12}$  neutrons/cm<sup>2</sup> and their leakage current is measured  
 to control if it remains below the allowed limit of 2 mA when  
 operating at low temperature,  $0^\circ\text{C}$ , and at reduced operating  
 voltages.

#### 127 4. Final electronics design

128 Each Mu2e-SiPM will be connected to its own Front End  
 129 Electronic board (FEE), which provides two gain amplification  
 130 stages ( $\times 3, \times 6$ ) and a linear regulation of the bias voltage. The  
 131 FEE also shapes the sensor signal to obtain a 25 ns long rise  
 132 time and a full signal width of 150 ns. The dynamic range is  
 133 0-2 V. The FEE board is also used to monitor the sensor tem-  
 perature and current.



Figure 6: Picture of the electronic board used to manage and read out 20 SiPM+FEE channels.

The FEE is managed and read out by a two stages digital board (Fig. 6), for a total of 20 channels per board. The

137 first stage, named Mezzanine Board (MB), provides setting and  
 138 reading of the bias voltage as well as a reading of temperature  
 139 and dark current. Moreover it receives the FEE differential sig-  
 140 nals in input that are then digitized in the second board stage  
 141 at 200 Msps with a 12 bit ADC. The second stage is composed  
 142 by a custom Digital Readout Controller board (DIRAC) based  
 143 on a very performing FPGA (MicroSemi PolarFire). A VTRX  
 144 optical link is used to readout the DIRAC board by the DAQ  
 145 system.

146 Radiation hardness tests have been performed by exposing  
 147 single boards or components both to a Total Ionization Dose  
 148 (TID) or to a neutron beam. After modification of few com-  
 149 ponents, the FEE boards showed to be radiation hard up to a  
 150 TID of 100 krad. The digital boards demonstrated to be able  
 151 to sustain a TID up to 30 krad, showing negligible deterio-  
 152 ration. Work is in progress to optimize the selection for the  
 153 DC-DC converter and to complete the test on the PolarFire  
 154 FPGA. The FEE boards were exposed to few MeV neutrons,  
 155 up to  $10^{12} \text{ n}_1 \text{ MeV/cm}^2$ ; no sign of deterioration was observed.  
 156 An additional set of tests with  $> 20 \text{ MeV/c}$  protons is planned  
 157 to evaluate the resistance of the digital boards to single event  
 158 upsets.

## 159 5. Final mechanics design

160 The engineering drawing of the Mu2e calorimeter is com-  
 161 pleted. Figure 7 shows an exploded view of a calorimeter disk.

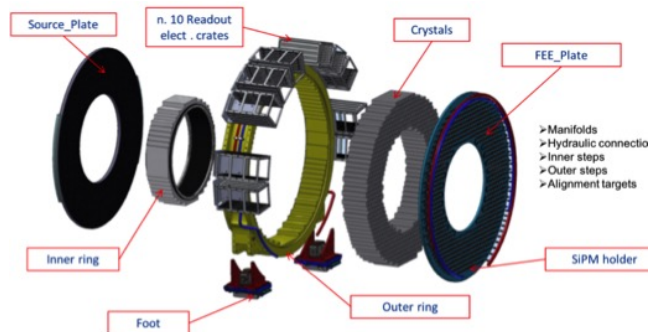


Figure 7: Exploded view of a calorimeter disk mechanic.

162 The main components are: the outer and the inner cylinders,  
 163 the PEEK FEE plate, which is needed to insert, cool down and  
 164 align the SiPMs and FEE to the corresponding crystals; the car-  
 165 bon fiber front face where the radioactive source pipes are in-  
 166 tegrated; the crates mounted on the external cylinder (10 per-  
 167 cent of the disk), where the digital electronics is located. A Finite  
 168 Element Analysis has been carried out, showing a good stability  
 169 of the system, with negligible stress on the supports. A full  
 170 dimension calorimeter mockup has been built and filled with  
 171 fake iron crystals to optimize the assembly procedure. Crystals  
 172 wrapped with  $150 \mu\text{m}$  Tyvek foils will be stacked from the bot-  
 173 tom to the top inside the external aluminum cylindrical support.  
 174 Finally, the calorimeter mechanical components have been in-  
 175 serted in the GEANT-4 simulation of the detector to control any  
 176

eventual offsets in cluster reconstruction. Negligible variation  
 in response and resolution is observed.

## 183 6. Conclusions

184 The Mu2e calorimeter is a state of the art crystal calorimeter  
 185 with excellent energy and timing performances for 105 MeV/c  
 186 electrons. A long R&D phase demonstrated that the chosen de-  
 187 sign largely satisfies the Mu2e requirements. Test beam results  
 188 of the large scale calorimeter prototype show that an energy re-  
 189 solution of about 7% and a time resolution better than 200 ps  
 190 are achievable with 100 MeV electrons impinging at 50 degrees.

191 The calorimeter production phase has started in March 2018  
 192 and is expected to be completed in October 2019. The readout  
 193 electronic design is now concluded and the FEE boards produc-  
 194 tion will start within a few months; the digital electronics pro-  
 195 duction will follow soon after. The calorimeter assembly will  
 start in November 2019 with the construction of the first disk.  
 The calorimeter installation in the Mu2e experimental hall is  
 planned for 2020, with a first commissioning phase done with  
 CRs data taking.

## 196 Acknowledgment

197 We are grateful for the vital contributions of the SEA and  
 198 BTF staff, Fermilab staff and the technical staff of the partic-  
 199 ipating institutions. This work was supported by the US  
 200 Department of Energy; the Italian Istituto Nazionale di Fisica  
 201 Nucleare; the Science and Technology Facilities Council, UK;  
 202 the Ministry of Education and Science of the Russian Feder-  
 203 ation; the US National Science Foundation; the Thousand Tal-  
 204 ents Plan of China; the Helmholtz Association of Germany; and  
 205 the EU Horizon 2020 Research and Innovation Program un-  
 206 der the Marie Skłodowska-Curie Grant Agreement No.690835.  
 207 This document was prepared by members of the Mu2e Collab-  
 208 oration using the resources of the Fermi National Accelerator  
 209 Laboratory (Fermilab), a U.S. Department of Energy, Office of  
 210 Science, HEP User Facility. Fermilab is managed by Fermi Re-  
 211 search Alliance, LLC (FRA), acting under Contract No. DE-  
 212 AC02-07CH11359.

- 213 [1] L.Bartoszek et al., (Mu2e experiment), *Mu2e Technical Design Report*  
 214 arXiv:1501.05241
- 215 [2] R.Donghia for the Mu2e Collaboration, *The Mu2e experiment at Fermi-*  
 216 *lab: Design and Status*, NC 40 C 176 (2017)
- 217 [3] N.Atanov et al., *The Mu2e Calorimeter Final Technical Design Report*,  
 218 arXiv:1802.06341
- 219 [4] N.Atanov et al., *Design and status of the Mu2e crystal calorimeter*, IEEE-  
 220 TNS, 10.1109/TNS.2018.2790702
- 221 [5] N.Atanov et al., *Design and status of the Mu2e electromagnetic calorime-*  
 222 *ter*, NIM A 824 (2016) 695
- 223 [6] O.Atanova et al., *Measurement of energy and time resolution of an un-*  
 224 *doped CsI + MPPC array for Mu2e experiment*, JINST 12 P05007 (2017)
- 225 [7] <http://www.lnf.infn.it/acceleratori/btf/>
- 226 [8] M.Cordelli et al., *Pre-production and quality assurance of the*  
 227 *Mu2e calorimeter Silicon Photomultipliers*, NIM A (2017),  
 228 DOI:10.1016/j.nima.2017.12.039
- 229 [9] N.Atanov et al., *Quality Assurance on un-doped CsI crystals for Mu2e*  
 230 *Experiment*, IEEE TNS 65 (2017) 752, DOI:10.1109/TNS.2017.2786081